Bioorganic & Medicinal Chemistry Letters 20 (2010) 7331–7336

Contents lists available at ScienceDirect

Bioorganic & Medicinal Chemistry Letters

journal homepage: www.elsevier.com/locate/bmcl

In silico identification and biochemical evaluation of novel inhibitors of NRH:quinone oxidoreductase 2 (NQO2)

Karen A. Nolan, Mary C. Caraher, Matthew P. Humphries, Hoda Abdel-Aal Bettley, Richard A. Bryce, Ian J. Stratford *

School of Pharmacy and Pharmaceutical Sciences, University of Manchester and Manchester Cancer Research Center, Manchester M13 9PT, UK

ARTICLE INFO

Article history:
Received 26 August 2010
Revised 14 October 2010
Accepted 14 October 2010
Available online 21 October 2010

Keywords:
NQO2
NQO1
Virtual screening
Molecular modeling
Inhibitors

ABSTRACT

The NCI chemical database has been screened using in silico docking to identify novel inhibitors of NRH:quinone oxidoreductase 2 (NQO2). Compounds identified from the screen exhibit a diverse range of scaffolds and inhibitory potencies are generally in the micromolar range. Some of the compounds also have the ability to inhibit NQO1. The modes of binding of the different compounds to the two enzymes are illustrated and discussed.

Quinone oxidoreductase 2 (NQO2, EC. 1.10.99.2) was first described by Liao and Williams-Ashmau in 1961[1] but was rediscovered by Jaiswal during the cloning of its homolog, NAD(P)H:quinone oxidoreductase 1 (NQO1, EC 1.6.99.2) in 1990.[2] The locus of the human gene for NQO2 has been mapped to chromosome 6p25 and is highly polymorphic.[3] The protein product has 231 amino acids and a molecular weight of 25,936 Da.[3] NQO2 is 43 residues shorter than NQO1 at the carboxy terminus and has a sequence identity of 54% for cDNA and 49% for protein.[3,4]

Human NQO2 is expressed in a variety of tissues including skeletal muscle, kidney, liver, lung and heart[5] but it does not appear to be induced in conjunction with NQO1.[6] Whereas the physiological role of NQO1 is reasonably well established, the biological function of NQO2 has yet to be determined.[7] Recent studies have shown that the genetic polymorphisms of NQO2 are associated with several neurological conditions, such as Schizophrenia,[8] Parkinson's disease[9] and Alzheimer's disease.[10]

The crystal structures of NQO1[11] and NQO2[12] show that the enzymes are very similar (Fig. 1).[7,11,12] Both proteins form homodimeric complexes with two active sites located at opposite ends of the dimer. Residues from both monomers line the active sites, which extend from the protein surface to the isoalloxazine rings of the bound FAD cofactors.[11,12] When the two structures are superimposed (Fig. 1C), the rmsd of the main chain Cα is 0.91 Å, with the active site residues aligned very well and the two FAD substituents virtually overlapping each other (Fig. 1D).[7,13] However, several key differences can be noted in the catalytic domains of the two enzymes.[7,12,13]

In NQO1, Tyr126 and Tyr128 are positioned in the active site with their side chains perpendicular to the plane of the FAD isoalloxazine ring.[12,1] These tyrosine residues are replaced by Phe126 and Ile128 in NQO2. Additionally, Met131 is replaced by Phe131 in NQO2.[12] Consequently, the binding pocket of NQO2 is slightly larger and more hydrophobic than NQO1.[12,13]

Tyr155 is involved in the catalytic cycle of NQO1 and is conserved in both enzymes. A proton is transferred from the OH of this residue to the O2F of FAD and the developing negative charge on Tyr155 is then directly stabilized by His161.[11] However, His161 is replaced by an asparagine residue in NQO2 and Asn161 is unable to stabilize a negative charge as a histidine does. Hence, the involvement of Asn161 in the catalytic cycle of NQO2 is unclear.[13] It was proposed that the zinc metal ion, which is unique to NQO2, maybe involved in catalysis.[6] However, recent studies have shown that the metal ion is most likely required for structural stability only.[13]

Whilst both enzymes can catalyze the two electron reduction of quinones, NQO1 uses NADH and NAD(P)H as electrons donors whereas NQO2 cannot use these co-substrates efficiently.[3,4] Instead NQO2 has been shown to use compounds derived from nicotinamide such as *N*-methyl-, *N*-benzyl or *N*-ribosyl-dihydronicotinamide (NRH).[14] The catalytic cycle of NQO1 and NQO2 is probably very similar, via the classic ping–pong mechanism. FAD is reduced by accepting a hydride from the reduced nicotinamide, to form the

* Corresponding author. Tel.: +44 161 275 2487; fax: +44 161 275 8342.
E-mail address: ian.stratford@manchester.ac.uk (I.J. Stratford).

0960-894X/$ - see front matter © 2010 Elsevier Ltd. All rights reserved.
doi:10.1016/j.bmcl.2010.10.070

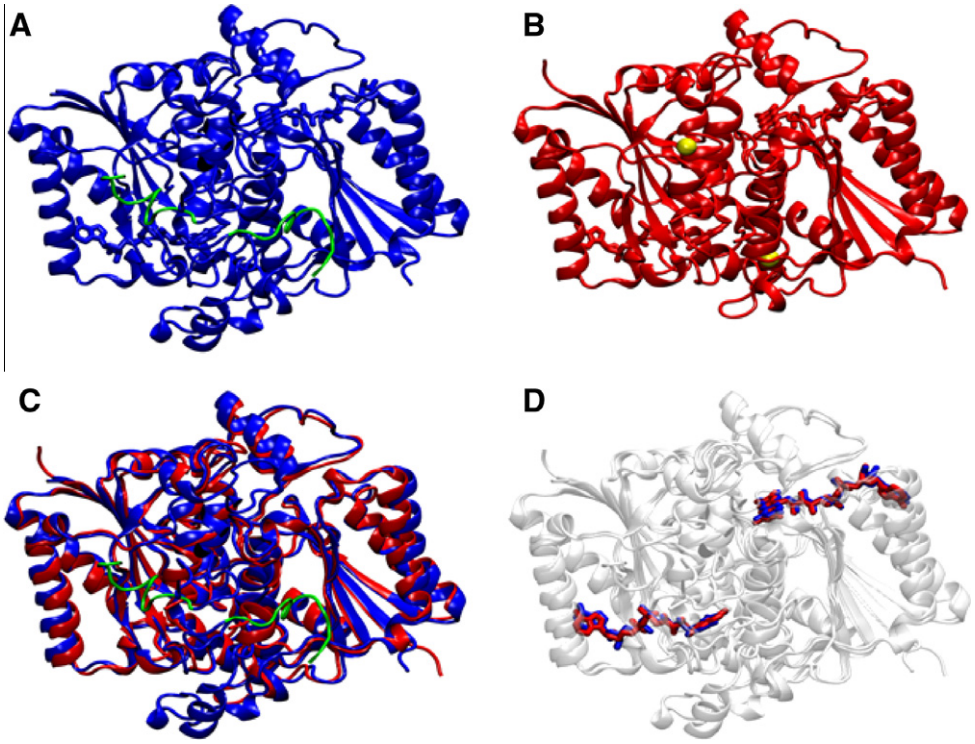

Figure 1. Ribbon representations of human NQO1 and NQO2 with FAD. (A) NQO1 with the FAD cofactor in blue and the C terminal regions from both monomers in green. (B) NQO2 with the FAD cofactor in red and the zinc atoms in yellow. (C) NQO1 (blue) and NQO2 (red) superimposed. (D) The FAD cofactors overlaid from NQO1 (blue) and NQO2 (red).

$FADH_2$-enzyme complex, after which the oxidized nicotinamide is released from the active site. The quinone then binds to the active site and subsequently accepts a hydride from $FADH_2$, thus completing the obligatory two electron reduction from nicotinamide to the quinone substrate.[11–13]

Besides the differences in the preference of electron donors for catalysis, NQO1 and NQO2 also have very different inhibitors.[6,7] The classical inhibitors of NQO1, such as dicoumarol and Cibracron Blue, do not significantly inhibit NQO2 activity.[6] Likewise, the well-characterized inhibitors of NQO2 such as resveratrol and quercetin only marginally inhibit NQO1 activity.[7] Another interesting variation between the in vivo activity of NQO1 and NQO2 is shown when animals with gene disruption demonstrate opposite properties towards menadione toxicity.[15] Animals with NQO2 gene disruption show increased resistance to quinone toxicity, whereas animals with NQO1 gene disruption demonstrate increased sensitivity to quinone toxicity.[15,16] Since both proteins share similarities in structure, catalytic mechanism and enzymatic activity towards menadione reduction, this presents a very fascinating paradox.[7]

We recently reported a virtual screening strategy to identify potential candidate ligands for NQO1.[17] This resulted in the discovery of the triazoloacrid-6-one, NSC645827, as a sub-micromolar inhibitor of NQO1.[17] As a consequence of this study, the NCI database was mined using a substructure screening approach to identify similar inhibitors within the database that were potential inhibitors of both NQO1 and NQO2.[18,19] From this study, the imidazoacridin-6-one NSC660841 was identified as one of the most potent inhibitors of NQO2 yet reported (IC_{50} = 6 nM).[19] In the present study, we have used a similar screening approach using the crystal structure of NQO2 to search the entire NCI database. This approach involved a hierarchical in silico screening of the National Cancer Institute database using computational molecular docking. This database contains over 700,000 compounds, most of which have been tested in a variety of biological screens, which helps in the search for novel ligands.[20]

For docking purposes, the crystallographic coordinates of the human NQO2 complex with bound FAD (PDB code 1QR2, resolution at 2 Å)[12] were obtained from the Brookhaven Data Bank. Hydrogen atoms were added to the structure allowing for appropriate ionization at physiological pH. The FAD fragment was reatom typed to avoid underestimation by ChemScore of lipophilic/aromatic interactions.[21] The protonated complex was then minimized within SYBYL 7.3 (Tripos, St. Louis, USA) whilst holding all heavy atoms stationary. Inspection of the active site showed a reasonable internal hydrogen bond network within the protein. The NCI database was docked using the genetic algorithm-based docking program, GOLD 3.2 in combination with the ChemScore scoring function.[22] The active site was defined as being any volume within 15 Å of N5 of the FAD cofactor. For the initial screen, GOLD library settings were selected and the top 25,000 highest scoring compounds were retained for further evaluation. These ligands were docked using the maximum number of operations permitted by GOLD to allow a thorough search for each compound. The top 1000 highest scoring ligands were visually inspected in the active site of NQO2 for the identification of favorable interactions and by pharmacokinetic considerations. A range of the 250 top-ranked ligands, were made available by the NCI and used for biochemical evaluation. Any compounds which were recognized as being commercially available were obtained from Sigma. All compounds were assessed for their enzymatic activity in NQO1 as well as NQO2. We report here the compounds identified as micromolar inhibitors of NQO2.

Recombinant human NQO1 and NQO2 were obtained from Sigma and diluted in 50 mM phosphate buffer to give an enzyme activity that would result in a change in optical absorbance of substrate of approximately 0.1 per minute. The enzyme reaction was started by adding 5 μL of this solution to 495 μL of 50 mM phosphate buffer at pH 7.4 containing 200 μM NADH or NRH, for NQO1 and NQO2, respectively, together with 40 μM dichlorophenolindophenol (DCPIP) and various concentrations of the potential

inhibitor dissolved in DMSO (final concentration 1.0% v/v). The DMSO concentration used is sufficiently small to ensure minimal perturbation of hydrogen bonding networks in aqueous NQO1 or NQO2 complexes. Reactions were carried out at 37 °C and reduction of DCPIP was monitored at 600 nm in a Beckman DU 650 spectrophotometer. IC_{50} values were determined using nonlinear curve fitting as implemented in the program Excel for which a 50% reduction of the initial rate was attained. Each measurement was made in triplicate and the experiments were carried out three times. IC_{50} values, given in Table 1, are derived from each of these determinations. Examples of inhibition curves are given in Figures 2 and 3. In all experiments, positive controls for enzyme inhibition were included. These were resveratrol for NQO2 and dicoumarol for NQO1. Typical curves for these agents are also given in Figures 2 and 3.

The calculated binding energies for all biochemically active compounds are given in Table 1. The docking studies suggest that the active site of NQO2 can accommodate ligands of different size and structure adopting a variety of binding modes and interactions. This is confirmed by the number of structurally diverse scaffolds which are given in Supplementary Table 1. **NSC86715** and **NSC238146** represent two commonly occurring scaffolds (based on ellipticine and quinoline, respectively) and these are shown in Figure 2. **NSC86715** has a calculated binding energy of 58.3 kJ/mol and an IC_{50} value of 2.1 μM for inhibition of NQO2.

This ligand is unable to form any polar contacts and is held in the active site of NQO2 by lipophilic interactions. Multiple hydrophobic contacts are formed between **NSC86715** and the isoalloxazine ring of FAD and the side chains of Trp105′, Phe106′, Leu120,

Table 1
NCI compounds, their chemical name (structures are given in Supplementary Table 1), GOLD binding energies and experimental IC_{50} values

NSC number	Chemical name	ΔGcalc[a] (kJ/mol)	NQO2[b] IC_{50} (μM)	NQO1[b] IC_{50} (μM)
27296	N^4-(6-Methoxy-8-quinolinyl)-1,4-pentanediamine; primaquine	−47.6	7.5 ± 2.75	
65069	[1,1′-Biphenyl]-2,3′,4,5′,6-pentol	−46.3 (−41.1)		10 ± 1.41
66167	[1,1′-Biphenyl]-2,2′,4,4′-tetrol	−50.9	5.8 ± 0.58	
77833	1-(2-(1*H*-Indol-3-yl)vinyl)isoquinoline	−59.7	1.8 ± 0.29	
78017	2,6-Dimethyl-3*H*-6λ^5-pyrrolo[3,2-*f*]quinoline	−58.8	2.1 ± 0.62	
78021	4,7-Dimethyl-7*H*-4λ^5-pyrido[2,3-*c*]carbazole	−55.4	5.5 ± 0.61	
86715	5-Methyl-1-phenyl-6*H*-pyrido[4,3-*b*]carbazole	−58.3	2.1 ± 0.38	
97374	1-Ethyl-2-((1-ethyl-2(1*H*)-quinolinylidene)methyl)-1λ^5-quinoline	−55.7	2.7 ± 0.17	
99495	3-Benzo[*a*]anthracen-12-ylthiophene	−53.1	5.1 ± 1.22	
99528	2-Benzo[*a*]anthracen-12-yl-1-benzothiophene	−54.2 (−56.8)	6.0 ± 1.07	1.1 ± 0.42
106080	Bis(2-hydroxyphenyl)methanone phenylhydrazone	−49.1 (−50.4)	3.9 ± 0.49	3.0 ± 0.21
115890	1,3-Naphthalenediol	−40.2	3.3 ± 0.85	
180969	7,8-Dimethoxy-4-(3,4,5-trimethoxyphenyl)-1,2-dihydro-3H-benzo[*e*]isoindol-3-one	−50.5	2.0 ± 0.12	
187208	N^4-(7-Chloro-4-quinolinyl)-N^1,N^1-diethyl-1,4-pentanediamine; chloroquine	−49.8	1.5 ± 0.50	
204996	7,8-Dimethoxy-4-(3,4,5-trimethoxyphenyl)-2,3-dihydro-1*H*-benzo[*e*]isoindole	−54.4	2.7 ± 0.42	
238146	N^4-(6-((6-amino-2-methyl-4-quinolinyl)amino)hexyl)-2-methyl-4,6-quinolinediamine acetate	−64.2	1.9 ± 0.10	
300853	3-Amino-9-ethyl-2-((4-(hydroxy(oxido)amino)phenyl)diazenyl)-9*H*-carbazole	−57.5	5.0 ± 0.85	
306843	1-Methyl-4(1*H*)-quinolinone (1-methyl-4(1*H*)-quinolinylidene)hydrazone	−58.8	6.2 ± 0.80	
332172	2-(4-Methoxyphenyl)-3-(3,4,5-trimethoxyphenyl)acrylonitrile	−48.1 (−43.6)	20 ± 1.53	40 ± 10.50
356819	4-((2-Hydroxy-5-(phenyldiazenyl)phenyl)diazenyl)benzenecarboximidamide	−60.9	1.8 ± 0.78	
356820	4-((2-Hydroxy-5-(2-phenylvinyl)phenyl)diazenyl)benzenecarboximidamide	−61.3	1.4 ± 0.61	
359466	4-((4-(Amino(imino)methyl)phenyl)diazenyl)-3-hydroxy-*N*-phenyl-2-naphthamide	−59.3	6.0 ± 0.95	
381864	5-(2-(3,5-Dimethoxyphenyl)vinyl)-2-methoxyphenol	−46.1 (−43.9)	15 ± 3.79	80 ± 11.9
621351	2-(2-Fluorophenyl)-4-(2-naphthyl)-2,3-dihydro-1,5-benzothiazepine	−57.6 (−51.0)		0.39 ± 0.08
623234	3-Chloro-3-(3,4-dimethoxyphenyl)-2-(3,4,5-trimethoxyphenyl)acrylaldehyde	−51.0	22 ± 5.61	
640353	1-(2-(3,5-Diphenyl-1*H*-pyrazol-1-yl)-4-methyl-1,3-thiazol-5-yl)-4-methyl-5-phenyl-2,4-pentadien-1-one	−61.2	3.8 ± 0.81	
640556	1-(2-(3,5-Diphenyl-1*H*-pyrazol-1-yl)-4-methyl-1,3-thiazol-5-yl)-3-(4-(hydroxy(oxido)amino)phenyl)-2-propen-1-one	−58.9	6.0 ± 0.70	
640558	1-(2-(3,5-Diphenyl-1*H*-pyrazol-1-yl)-4-methyl-1,3-thiazol-5-yl)-3-phenyl-2-propen-1-one	−60.6	5.8 ± 0.85	
640559	1-(2-(3,5-Diphenyl-1*H*-pyrazol-1-yl)-4-methyl-1,3-thiazol-5-yl)-3-(3-(hydroxy(oxido)amino)phenyl)-2-propen-1-one	−62.3	6.5 ± 1.58	
640566	3-(4-Chlorophenyl)-1-(2-(3,5-diphenyl-1*H*-pyrazol-1-yl)-4-methyl-1,3-thiazol-5-yl)-2-propen-1-one	−58.2	5.3 ± 0.67	
640583	1-(2-(3,5-Diphenyl-1*H*-pyrazol-1-yl)-4-methyl-1,3-thiazol-5-yl)-3-(4-methylphenyl)-2-propen-1-one	−60.7	3.2 ± 0.85	
640584	3-(3,4-Dichlorophenyl)-1-(2-(3,5-diphenyl-1*H*-pyrazol-1-yl)-4-methyl-1,3-thiazol-5-yl)-2-propen-1-one	−61.4	4.9 ± 0.29	
648420	1,2,3-Trimethoxyphenanthro[2,3-*d*][1,3]dioxol-6-yl acetate	−44.7 (−47.9)		70 ± 2.83
648422	5-(1-Methyl-2-(3,4,5-trimethoxyphenyl)vinyl)-1,3-benzodioxole	−48.5 (−45.5)		55 ± 7.64
649091	2-((Diethylamino)methyl)-4-((10-methyl-10*H*-indolo[3,2-*b*]quinolin-11-yl)amino)phenol hydrochloride	−61.6	3.5 ± 1.26	
665126	1-(2-(4-(Hydroxy(oxido)amino)phenyl)vinyl)-3-phenylbenzo[*f*]quinoline	−60.7	9.6 ± 0.58	
669977	6-Imino-1-methyl-3-phenyl-2,6-dihydro-5(1*H*)-quinolinone hydrazone	−57.5	2.0 ± 0.70	
676468	*N*-(3-([1,1′-Biphenyl]-4-ylimino)-1-propenyl)[1,1′-biphenyl]-4-amine	−52.9	9.7 ± 0.46	
677939	14*H*-Diindolo[2,3-*a*:3,2-*h*]quinolizine	−61.5	2.9 ± 0.10	
693571	Trifluoromethanesulfonic acid compound with *N*,*N*-dimethyl-4-((1-methyl-2-phenyl-4*H*-1λ^5-pyrazolo[1,5-*a*]indol-4-ylidene)methyl)aniline	−62.2	1.7 ± 0.25	
720622	Trifluoromethanesulfonic acid compound with *N*,*N*-dimethyl-4-(1-methyl-6-nitro-2-phenylpyrazolo[1,5-*a*]indol-1-ium-4-ylidene)methyl]aniline	−59.7	5.0 ± 1.10	

[a] Values in parentheses are the binding energies calculated for NQO1.
[b] The blanks indicate no inhibition at 100 μM.

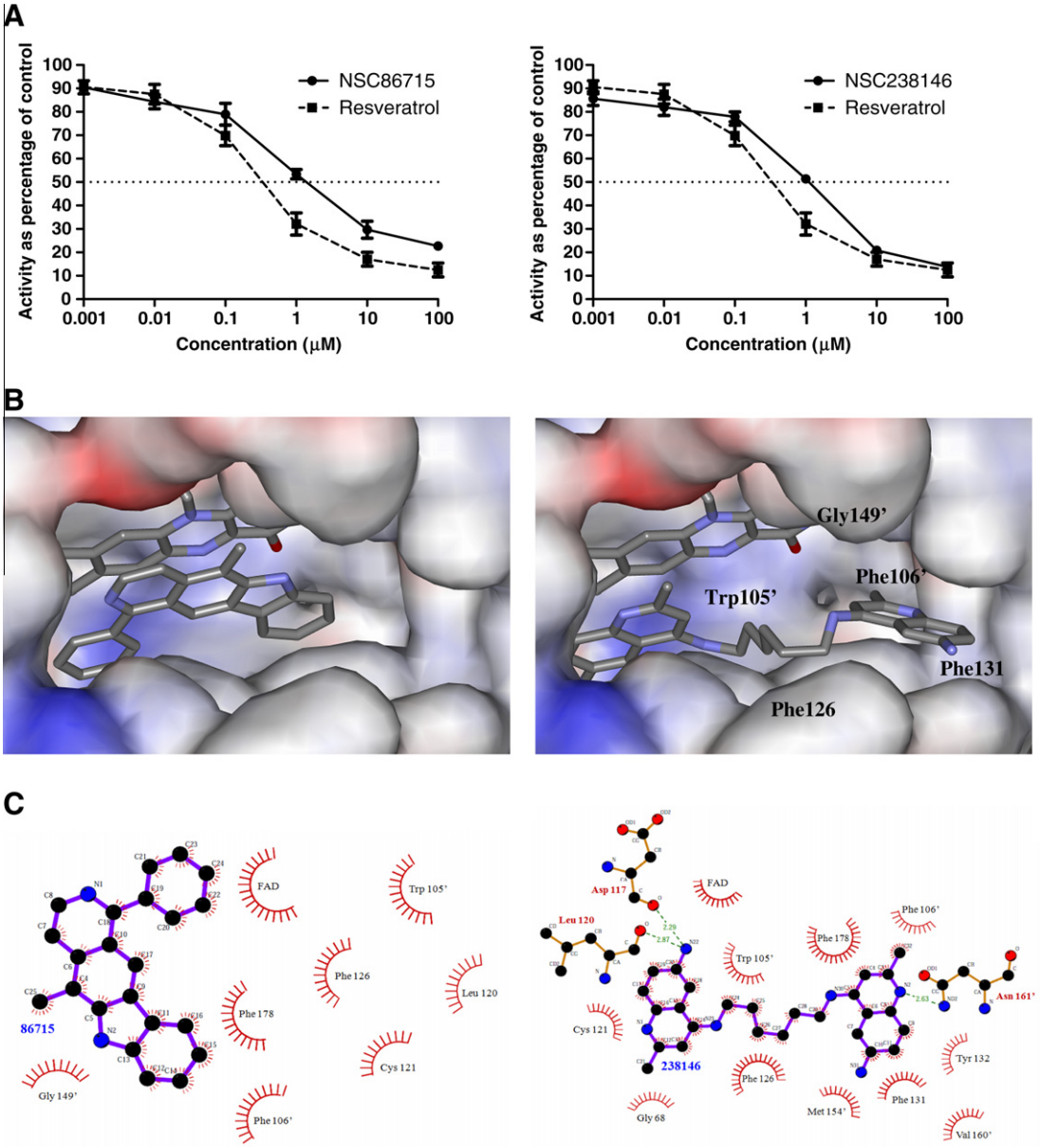

Figure 2. Left panels **NSC86715**, right panels **NSC238146**. (A) Enzyme (NQO2) inhibition curves for both compounds; data points indicate mean values ± standard deviations from three independent experiments (●). Also shown are inhibition curves for the known inhibitor resveratrol (■). (B) Electrostatic surface representations with **NSC86715** and **NSC238146** in the binding pocket of NQO2. Also shown is the proximity of the FAD cofactor which allows π overlap with the inhibitors. In addition the location of key amino acids within the surface representation are given (right panel). (C) LigPlot[24] representations of inhibitor/NQO2 interactions. Nitrogen atoms are colored in blue, oxygen atoms are colored in red, and carbon atoms are colored in black. Hydrogen bonds are represented by dashed green lines along with their distances. Residues making hydrogen bonds together with inhibitor are shown in stick representation. Residues making van der Waals interactions with the inhibitors are represented by a decorated arc. Amino acids in the active site from the different monomers are indicated with and without the prime symbol.

Cys121, Phe126, Gly149′ and Phe178 (Fig. 2C). **NSC238146** is the highest scoring compound in this series with a calculated binding energy of 64.2 kJ/mol and an IC_{50} value of 1.9 μM for inhibition of NQO2. This ligand forms close hydrogen bond contacts with Asn161′ (2.63 Å), Asp117 (2.29 Å) and Leu120 (2.87 Å) as well as lipophilic interactions with the isoalloxazine ring of FAD and active site residues; Gly68, Trp105′, Phe106′, Cys121, Phe126, Phe131, Tyr132, Met154′, Val160′ and Phe178 (Fig. 2C).

Interestingly, the antimalarial quinolines, **NSC27296** (Primaquine) and **NSC187208** (Chloroquine) were also identified from the in silico screen with binding energies of 47.6 kJ/mol and 49.8 kJ/mol, respectively. **NSC27296** has an IC_{50} value of 7.5 μM and **NSC187208** has an IC_{50} value of 1.5 μM.

The active site of NQO2 is a cavity, 17 Å in length and 7 Å wide, which is ideal in shape for receiving a variety of polycyclic and polyaromatic compounds, the diversity of which is shown in Supplementary Table 1. Many of these compounds including, **NSC356419**, **NSC356420**, **NSC640353**, **NSC640556**, **NSC640558**, **NSC640559**, **NSC640566**, **NSC640583** and **NSC640584** exclusively inhibited NQO2 but showed no ability to inhibit NQO1 at concentrations up to 100 μM. In contrast, four compounds (**NSC99528**, **NSC106080**, **NSC332172** and **NSC381864**) were found to be active against both NQO2 and NQO1. On the contrary, **NSC65069**, **NSC621351**, **NSC648420** and **NSC648422** were found to inhibit NQO1 but not NQO2 (Table 1) although they were identified from the NQO2 screen. These eight compounds were subsequently docked into the active site of NQO1 and their binding energies are given in Table 1. **NSC621351** is the most potent inhibitor of NQO1 with an IC_{50} value of 390 nM and a binding energy of 51.0 kJ/mol (Fig. 3). This ligand is shown to bind deep in the active

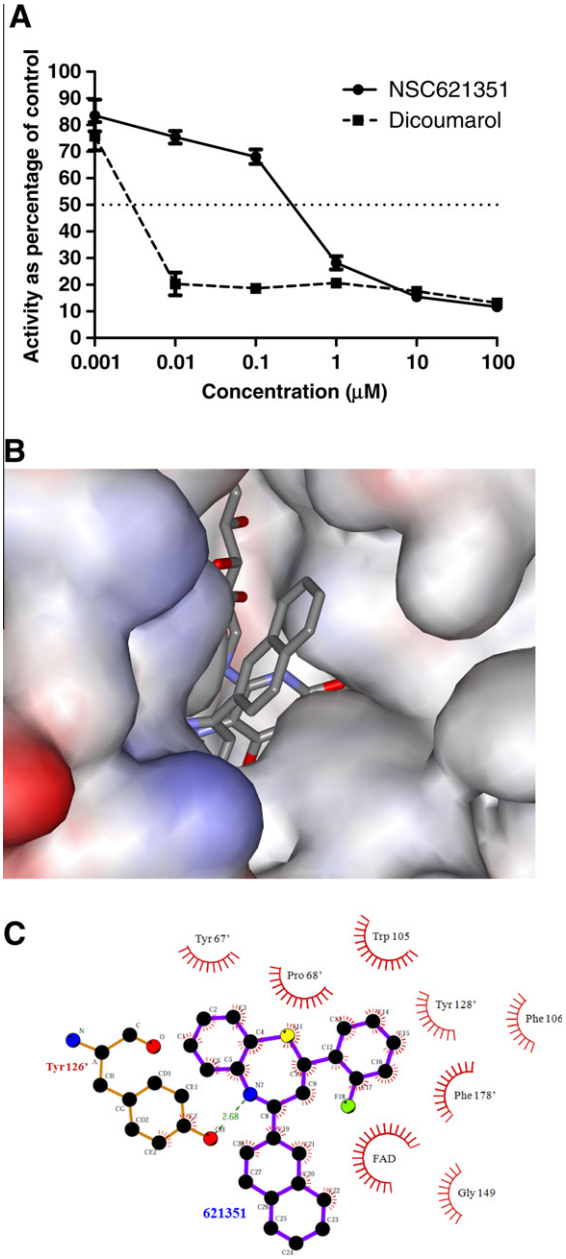

Figure 3. (A) Enzyme (NQO1) inhibition curve for **NSC621351** (●); also shown is the inhibition curve for the known inhibitor dicoumarol (■). Data points indicate mean values ± standard deviations from three independent experiments. (B) Electrostatic surface representation with **NSC621351** in the binding pocket of NQO1. Also shown is the proximity of the FAD cofactor which allows π overlap with the inhibitor. (C) LigPlot[24] representations of the interaction between **NSC621351** and NQO1. Nitrogen atoms are colored in blue, oxygen atoms are colored in red, and carbon atoms are colored in black. Hydrogen bonds are represented by dashed green lines along with their distances. Residues making hydrogen bonds together with inhibitor are shown in stick representation. Residues making van der Waals interactions with the inhibitors are represented by a decorated arc. Amino acids in the active site from the different monomers are indicated with and without the prime symbol.

site of NQO1 and forms a close hydrogen bond contact with Tyr126′ (2.68 Å) as well as lipophilic interactions with the isoalloxazine ring of FAD and the side chains of Tyr67′, Pro68′, Trp105, Phe106, Tyr128′, Gly149 and Phe178′ (Fig. 3C). The active site of NQO1 is composed of two distinct but joined pockets, previously described as the 'FAD pocket' and a second frontal 'access pocket'.[21] This is clearly shown for **NSC621351** which has most of the ligand buried in the FAD pocket, but the 2-naphthyl ring is apparent in the access pocket of the active site of NQO1 (Fig. 3B).

No clear correlation could be established between the calculated binding affinities for ligands with NQO2 and experimentally determined IC_{50} values for the compounds evaluated in this screen. This is most likely to be a consequence of the structurally diverse scaffolds that have been identified and this has previously been the case for NQO1.[17] However, our previous work has also shown that, within structural classes such as triazoloacridin-6-ones and imidazoacridine-6-ones, strong structure–activity relationships can be obtained relating calculated and experimentally determined binding energies, (correlation coefficients ~0.9).[18,19,21,23]

Among the compounds identified from the NCI screen were some that showed no ability to inhibit NQO2 (or NQO1) at concentrations up to 100 μM, despite having binding energies as high as 63.9 kJ/mol. These compounds are listed in Supplementary Table 2. Whilst it is disappointing to obtain some false positives using our screening strategy, it does provide opportunities for refining our computational methodologies in order to improve the predictive power of our approach.

In conclusion, we have used virtual screening of the NCI chemical database to identify inhibitors of NQO2 that are active in the micromolar range. These agents represent a variety of structural types that should provide the basis for development of more potent inhibitors of this enzyme. In addition, we have illustrated the structural similarities and differences between NQO2 and NQO1. From the screen of potential NQO2 inhibitors, we identified some compounds that were also effective against NQO1. This property has only been seen previously in a series of triazoloacridin-6-ones[23] and therefore may provide additional scope for drug development.

Acknowledgements

This work is supported by an MRC program grant to I.J.S. (G0500366) and a project grant from the AICR (I.J.S., R.B. and K.A.N.). We thank the Drug Synthesis and Chemistry Branch, Developmental Therapeutics Program, Division of Cancer Treatment and Diagnosis, NCI for the supply of compounds.

Supplementary data

Supplementary data associated with this article can be found, in the online version, at doi:10.1016/j.bmcl.2010.10.070.

References and notes

1. Liao, S.; Williams-Ashmau, H. G. *Biochem. Biophys. Res. Commun.* **1961**, *4*, 208.
2. Jaiswal, A. K.; Burnett, P.; Adesnik, M.; McBride, O. W. *Biochemistry* **1990**, *29*, 1899.
3. Long, D. J., II; Jaiswal, A. K. *Gene* **2000**, *252*, 107.
4. Long, D. J., II; Jaiswal, A. K. *Chem. Biol. Interact.* **2000**, *129*, 99.
5. Jaiswal, A. K. *J. Biol. Chem.* **1994**, *269*, 14502.
6. Zhao, Q.; Yang, X. L.; Holtclaw, W. D.; Talalay, P. *Proc. Natl. Acad. Sci. U.S.A.* **1997**, *94*, 1669.
7. Fu, Y.; Buryanovskyy, L.; Zhang, Z. *Biochem. Biophys. Res. Commun.* **2005**, *336*, 332.
8. Harada, S.; Tachikawa, H.; Kawanishi, Y. *Psychiatr. Genet.* **2003**, *13*, 205.
9. Wang, W.; Le, W. D.; Pan, T.; Stringer, J. L.; Jaiswal, A. K. *J. Gerontol. A Biol. Sci. Med. Sci.* **2008**, *63*, 127.
10. Brouillette, J.; Quirion, R. *Neurobiol. Aging* **2008**, *29*, 1721.
11. Faig, M.; Bianchet, M. A.; Talalay, P.; Chen, S.; Winski, S.; Ross, D.; Amzel, L. M. *Proc. Natl. Acad. Sci. U.S.A.* **2000**, *97*, 3177.
12. Foster, C. E.; Bianchet, M. A.; Talalay, P.; Zhao, Q.; Amzel, L. M. *Biochemistry* **1999**, *38*, 9881.
13. Buryanovskyy, L.; Fu, Y.; Boyd, M.; Ma, Y.; Hsieh, T. C.; Wu, J. M.; Zhang, Z. *Biochemistry* **2004**, *43*, 11417.
14. Knox, R. J.; Jenkins, T. C.; Hobbs, S. M.; Chen, S.; Melton, R. G.; Burke, P. J. *Cancer Res.* **2000**, *60*, 4179.
15. Long, D. J.; Gaikwad, A.; Multani, A.; Pathak, S.; Montgomery, C. A.; Gonzalez, F. J.; Jaiswal, A. K. *Cancer Res.* **2002**, *62*, 3030.

16. Long, D. J., II; Iskander, K.; Gaikwad, A.; Arin, M.; Roop, D. R.; Knox, R.; Barrios; Jaiswal, A. K. *J. Biol. Chem.* **2002**, *277*, 46131.
17. Nolan, K. A.; Timson, D. J.; Stratford, I. J.; Bryce, R. A. *Bioorg. Med. Chem. Lett.* **2006**, *16*, 6246.
18. Nolan, K. A.; Zhao, H.; Faulder, P. F.; Frenkel, A. D.; Timson, D. J.; Siegel, D.; Ross, D., ; Burke, T. R., Jr.; Stratford, I. J.; Bryce, R. A. *J. Med. Chem.* **2007**, *50*, 6316.
19. Nolan, K. A.; Humphries, M. P.; Bryce, R. A.; Stratford, I. J. *Bioorg. Med. Chem. Lett.* **2010**, *20*, 2832.
20. Fitzsimmons, S. A.; Workman, P.; Grever, M.; Paull, K.; Camalier, R.; Lewis, A. D. *J. Natl. Cancer Inst.* **1996**, *8*, 259.
21. Nolan, K. A.; Doncaster, J. R.; Dunstan, M. S.; Scott, K. A.; Frenkel, A. D.; Siegel, D.; Ross, D.; Barnes, J.; Levy, C.; Leys, D.; Whitehead, R. C.; Stratford, I. J.; Bryce, R. A. *J. Med. Chem.* **2009**, *52*, 7142.
22. Verdonk, M. L.; Cole, J. C.; Hartshorn, M. J.; Murray, C. W.; Taylor, R. D. *Proteins* **2003**, *52*, 1028.
23. Nolan, K. A.; Humphries, M. P.; Barnes, J.; Doncaster, J. R.; Caraher, M. C.; Tirelli, N.; Bryce, R. A.; Whitehead, R. C.; Stratford, I. J. *Bioorg. Med. Chem.* **2010**, *18*, 696.
24. Wallace, A. C.; Laskowski, R. A.; Thornton, J. M. *Protein Eng.* **1995**, *8*, 127.